Regulator of G protein signaling 2 mediates cardiac compensation to pressure overload and antihypertrophic effects of PDE5 inhibition in mice

Eiki Takimoto,[1] Norimichi Koitabashi,[1] Steven Hsu,[1] Elizabeth A. Ketner,[1] Manling Zhang,[1] Takahiro Nagayama,[1] Djahida Bedja,[2] Kathleen L. Gabrielson,[2] Robert Blanton,[3] David P. Siderovski,[4] Michael E. Mendelsohn,[3] and David A. Kass[1]

[1]Division of Cardiology, Department of Medicine, and [2]Department of Comparative Medicine and Comparative Pathology, Johns Hopkins University School of Medicine, Baltimore, Maryland, USA. [3]Molecular Cardiology Research Institute, Tufts–New England Medical Center and Tufts University School of Medicine, Boston, Massachusetts, USA. [4]Department of Pharmacology, University of North Carolina, Chapel Hill, North Carolina, USA.

The heart initially compensates for hypertension-mediated pressure overload by enhancing its contractile force and developing hypertrophy without dilation. G_q protein–coupled receptor pathways become activated and can depress function, leading to cardiac failure. Initial adaptation mechanisms to reduce cardiac damage during such stimulation remain largely unknown. Here we have shown that this initial adaptation requires regulator of G protein signaling 2 (RGS2). Mice lacking RGS2 had a normal basal cardiac phenotype, yet responded rapidly to pressure overload, with increased myocardial G_q signaling, marked cardiac hypertrophy and failure, and early mortality. Swimming exercise, which is not accompanied by G_q activation, induced a normal cardiac response, while *Rgs2* deletion in $G_{\alpha q}$-overexpressing hearts exacerbated hypertrophy and dilation. In vascular smooth muscle, RGS2 is activated by cGMP-dependent protein kinase (PKG), suppressing G_q-stimulated vascular contraction. In normal mice, but not *Rgs2*$^{-/-}$ mice, PKG activation by the chronic inhibition of cGMP-selective phosphodiesterase 5 (PDE5) suppressed maladaptive cardiac hypertrophy, inhibiting G_q-coupled stimuli. Importantly, PKG was similarly activated by PDE5 inhibition in myocardium from both genotypes, but PKG plasma membrane translocation was more transient in *Rgs2*$^{-/-}$ myocytes than in controls and was unaffected by PDE5 inhibition. Thus, RGS2 is required for early myocardial compensation to pressure overload and mediates the initial antihypertrophic and cardioprotective effects of PDE5 inhibitors.

Introduction

The adult heart responds to sustained pressure overload by developing ventricular hypertrophy. The signaling events mediating this process are substantially driven by activation of GPCRs, which in turn stimulate multiple downstream intracellular cascades. Exposure to sufficient magnitude and duration of GPCR stimulation is thought to be necessary to tip the balance between adaptive and maladaptive responses (1, 2). However, the response may also depend upon how well the heart can mount countermeasures to effectively blunt such adverse signaling.

One set of negative controllers of GPCRs is the family of more than 30 regulator of G protein signaling (RGS) proteins (3). Upon GPCR activation, GDP is exchanged for GTP on the G_α subunit, allowing for dissociation from $G_{\beta\gamma}$ subunits and activation of downstream effectors. RGS proteins inhibit these cascades by accelerating G_α-dependent GTP hydrolysis to reconstitute the heterotrimeric G protein complex. RGS proteins also act as effecter antagonists by physically blocking the binding of G protein subunits to their protein targets and interfering with downstream signaling proteins (4). RGS2–RGS5 are thought to be important in the heart (5, 6), although their precise roles remain unclear. Human heart failure is associated with increased RGS4 expression, whereas expression of RGS2 is unchanged (7). Forced overexpression of RGS4 blunts G_q-stimulated cardiac hypertrophy in rat neonatal cardiac myocytes (8) and intact hearts (9) and suppresses cardiac hypertrophy of transgenic mice lacking guanylate cyclase–A (natriuretic peptide-stimulated cyclase; ref. 10). Yet other studies in hearts overexpressing RGS4 found rapid cardiac dilation and marked mortality upon pressure overload induction (11), highlighting a complex role. This was further demonstrated by the recent discovery that RGS4 regulates parasympathetic ($G_{\alpha[i/o]}$) signaling to control heart rate in the sinoatrial node (12).

In contrast to RGS4, which inactivates multiple G_α proteins (13), myocyte RGS2 appears more selective for $G_{\alpha q}$ (6, 14). Given the recognized and prominent role of G_q signaling to maladaptive remodeling as a result of pressure overload (15, 16), RGS2 is an intriguing candidate as an intrinsic suppressor of this pathobiology. Mice globally lacking RGS2 were found to develop modest systemic hypertension, although they exhibit no major cardiac phenotype (17), which suggested that RGS2 had a modest role in the heart. Yet more recent studies found that knockdown of the gene encoding RGS2 amplifies hypertrophic responses in neonatal myocytes exposed to G_q stimuli (18).

Authorship note: Norimichi Koitabashi and Steven Hsu contributed equally to this work.

Conflict of interest: The authors have declared that no conflict of interest exists.

Nonstandard abbreviations used: CaMKII, Ca^{2+}-calmodulin–dependent kinase II; Cn, calcineurin; ET1, endothelin-1; FS, fractional shortening; PDE5, phosphodiesterase 5; PLCβ, phospholipase Cβ; PV, pressure-volume; RGS, regulator of G protein signaling; TAC, transverse aortic constriction.

Citation for this article: *J. Clin. Invest.* **119**:408–420 (2009). doi:10.1172/JCI35620.

An important feature of both RGS2 and RGS4 is that they are activated by PKG, attenuating G_q-coupled vasoconstriction in vascular (19) and gastric (20) smooth muscle, and, in the case of RGS4, enhancing antihypertrophic effects of natriuretic peptides (10). Even more pronounced suppression of cardiac hypertrophy coupled to PKG activation has been achieved by inhibiting phosphodiesterase 5 (PDE5; ref. 21) with drugs widely used to treat erectile dysfunction (e.g., sildenafil). Given its greater selectivity for G_q, we hypothesized that RGS2 plays a particularly central role in the antihypertrophic effects of this therapy. Understanding such mechanisms has taken on clinical relevance, given the recently initiated NIH multicenter trial of the PDE5 inhibitor sildenafil for treating heart failure with a normal ejection fraction (RELAX study; http://clinicaltrials.gov/ct2/show/NCT00763867).

In the present study, we tested the role of RGS2 in pressure overload remodeling and its amelioration by PDE5 inhibition. Mice genetically lacking RGS2 did not compensate against pressure overload, but instead developed rapid and marked cardiac hypertrophy and dysfunction and early lethality. In contrast, their response to swimming exercise was normal. In addition to targeting myocardial G_q signaling, RGS2 was found to be essential in order for PDE5 inhibition to reduce hypertrophy and improve cardiac function upon exposure to pressure overload.

Results

RGS2 is expressed in adult mouse myocytes and suppresses G_q stimulation. RGS2 protein expression was detected in isolated adult myocytes from control *Rgs2*$^{+/+}$, but not *Rgs2*$^{-/-}$, mouse hearts (Figure 1A). RGS2-mediated protection against myocyte hypertrophy has been previously reported in neonatal myocytes using RGS2 RNAi (18). Here, we examined adult myocytes from *Rgs2*$^{+/+}$ and *Rgs2*$^{-/-}$ mouse hearts and found enhanced protein synthesis in cells incubated with the G_q agonist endothelin-1 (ET1). This finding supports the role of RGS2 in countering such stimulation in adult cells.

Rgs2$^{-/-}$ *mouse hearts develop marked hypertrophy and failure and early lethality from pressure overload.* To test whether RGS2 is cardioprotective against development of hypertrophy in vivo, *Rgs2*$^{-/-}$ mice (4–5 months old) were subjected to pressure overload by transverse aortic constriction (TAC; ref. 21). Resting cardiac anatomy and global function, as assessed by echocardiography, was similar between *Rgs2*$^{-/-}$ and littermate control *Rgs2*$^{+/+}$ mice (Supplemental Table 1; supplemental material available online with this article; doi:10.1172/JCI35620DS1). After TAC, however, *Rgs2*$^{-/-}$ mice developed marked hypertrophy (Figure 1C) and had a high mortality rate within 1 wk, whereas all *Rgs2*$^{+/+}$ mice survived this period (Figure 1D). Marked lung congestion (wet lung weight) was documented in surviving and deceased *Rgs2*$^{-/-}$ animals (Figure 1E), which supported heart failure as the cause of death. The increased heart mass was caused by both exacerbated myocyte hypertrophy and fibrosis (Figure 1F). Cardiac apoptosis was not observed within this 1-wk time period in either genotype (data not shown). TAC-induced changes in cardiac fetal genes *Nppa*, *Nppb*, and *Myh7* were greater in *Rgs2*$^{-/-}$ than in *Rgs2*$^{+/+}$ hearts, whereas expression of *Atp2a2* declined in both models similarly (Supplemental Figure 1).

Chamber dilation and lack of functional compensation in Rgs2$^{-/-}$ *TAC mouse hearts.* *Rgs2*$^{-/-}$ hearts dilated after pressure overload, with end-diastolic and end-systolic dimensions increasing and fractional shortening (FS) declining more than in *Rgs2*$^{+/+}$ hearts (Figure 2A). These echocardiographic data were supported by more detailed invasive pressure-volume (PV) analysis (Figure 2, B–D). At rest, *Rgs2*$^{-/-}$ mice had LV peak systolic pressure that was increased about 15 mmHg compared with *Rgs2*$^{+/+}$ mice and increased total LV afterload, as measured by effective arterial elastance (Figure 2C). However, basal cardiac systolic and diastolic function was essentially identical between the groups (Supplemental Table 2). TAC increased cardiac afterload to near-identical levels in both genotypes (Figure 2C), because load largely depended on the proximal aortic constriction. Similarities of loading changes after 48 h TAC were also confirmed (Supplemental Figure 2). In *Rgs2*$^{+/+}$ mice, 1 wk TAC triggered functional compensation with enhanced contractility: the end-systolic PV relation shifted leftward with increased slope (Figure 2B). This did not occur in *Rgs2*$^{-/-}$ mice; instead, hearts dilated with a rightward shift of PV relations (Figure 2B). Summary data for contractility (end-systolic PV relation slope, volume position, peak rate of LV pressure rise, and preload recruitable stroke work) and relaxation (peak rate of LV pressure decline and time constant tau) are provided in Figure 2D. Unlike control hearts, *Rgs2*$^{-/-}$ hearts failed to compensate by increasing contractility and had impaired relaxation, with net cardiac output depending more on marked chamber dilation (Frank-Starling law).

Early and robust activation of G_q-related pathways in Rgs2$^{-/-}$ *TAC mouse hearts.* Because RGS2 principally suppresses G_q signaling, we examined the activation of the phosphatase calcineurin (Cn), Ca^{2+}-calmodulin–dependent kinase II (CaMKII), and the MAPKs ERK1/2, JNK, and p38, all of which are potentially activated by G_q-coupled stimuli and are associated with hypertrophy and/or cardiac dilation (2, 22). After 1 wk TAC, Cn protein expression rose modestly in *Rgs2*$^{+/+}$ hearts, but markedly increased in *Rgs2*$^{-/-}$ hearts (Figure 3A). Parallel changes were observed in the gene expression of regulator of Cn-1 (RCAN-1), an index of Cn activity (Figure 3B). This was observed even after 48 h TAC in *Rgs2*$^{-/-}$ hearts, a time at which expression was otherwise unaltered. CaMKII activation also markedly increased after 48 h TAC in *Rgs2*$^{-/-}$ hearts and persisted at 1 wk TAC, whereas TAC *Rgs2*$^{+/+}$ hearts showed minimal CaMKII activation (Figure 3C). Among the 3 MAPKs, we observed greater activation of ERK1/2 and JNK at both time points in *Rgs2*$^{-/-}$ hearts (Figure 3D). Phosphorylation of p38 rose markedly and similarly in both groups after 48 h TAC, but declined at 1 wk TAC, which suggests that it was regulated by alternative cascades. These early signaling responses were not coupled to changes in RGS2 expression in control myocardium or myocytes (data not shown).

G_q is a critical target of RGS2. To test whether G_q is indeed the critical target of RGS2 in the heart, we performed several studies whereby G_q signaling was modified. Activation of phospholipase Cβ (PLCβ) is a primary mechanism for $G_{\alpha q}$ signaling and is required for dilated cardiomyopathy to develop in cardiac-targeted $G_{\alpha q}$-overexpressing transgenic animals (referred to herein as $G_{\alpha q}$-OE$^+$; ref. 23). We therefore subjected *Rgs2*$^{-/-}$ hearts to 48 h TAC with or without cotreatment by a PLCβ inhibitor (U73122, 2.5mg/kg/d) or inactive control (U73343). Exacerbated LV hypertrophy, chamber dilation, and dysfunction were observed after 48 h TAC in *Rgs2*$^{-/-}$ mice, and all were prevented in animals receiving the PLCβ inhibitor, whereas the inactive analog at the same dose had no impact (Figure 4, A and B; see Supplemental Figure 2B for summary echo data).

In a second series of experiments, $G_{\alpha q}$-OE$^+$ mice (24) were bred with *Rgs2*$^{-/-}$ animals, and cardiac function and morphology were examined at 3–4 wk of age. $G_{\alpha q}$-OE$^+$*Rgs2*$^{+/+}$ mice exhibited minimal hypertrophy, but slight chamber dilation and reduced FS. However, these 3 were substantially worsened in $G_{\alpha q}$-OE$^+$*Rgs2*$^{-/-}$ mice (Figure 4, C–E).

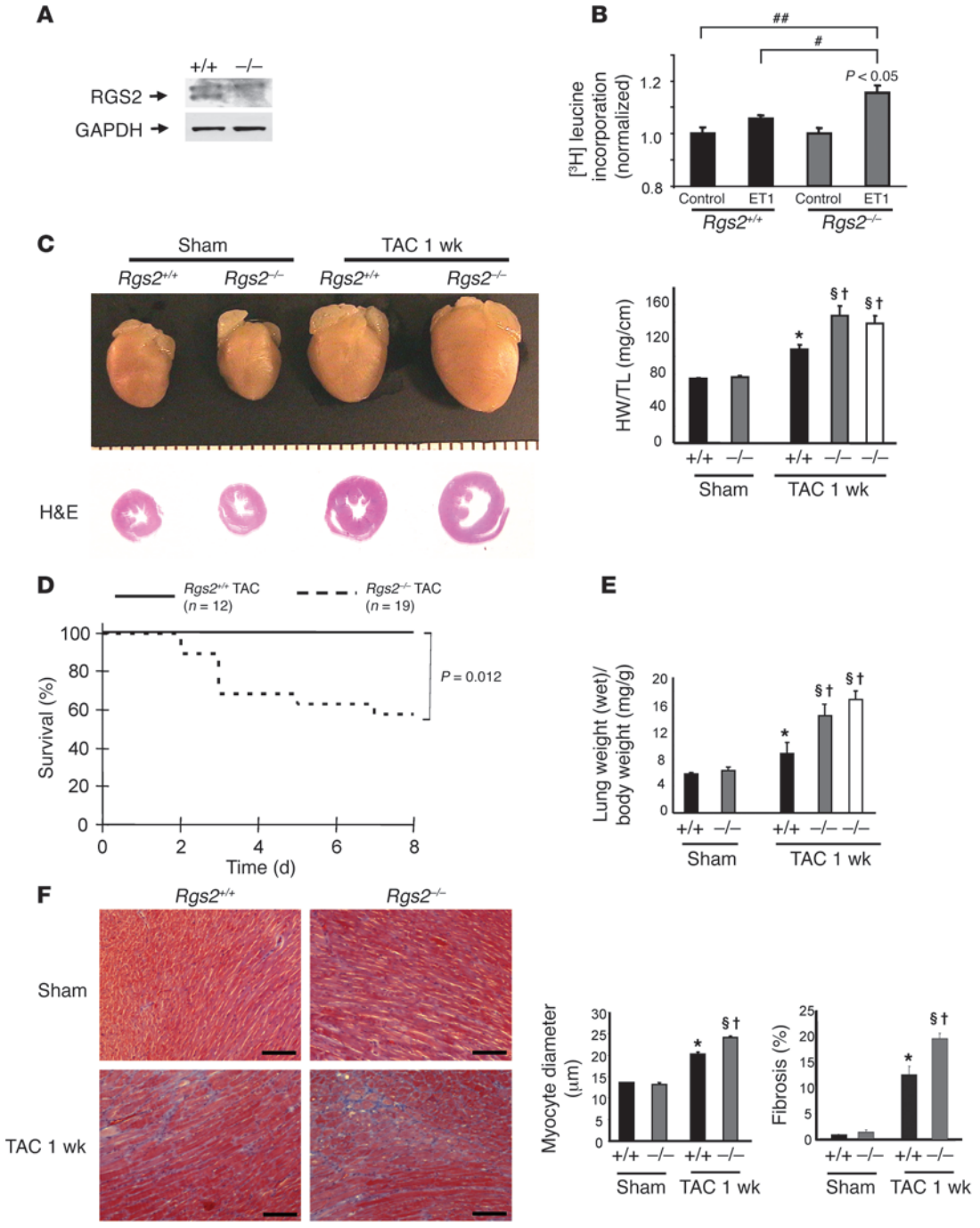

Figure 1

Cardiac phenotype of *Rgs2*$^{-/-}$ mice. (**A**) Myocyte RGS2 protein expression was detected in *Rgs2*$^{+/+}$ (+/+) cells, but not *Rgs2*$^{-/-}$ (–/–) cells. (**B**) Adult mouse myocytes (n = 5 per group) from *Rgs2*$^{-/-}$ hearts displayed an amplified growth response to ET1, as assessed by radiolabeled leucine incorporation. P value shown is for interaction of genotype and condition (2-way ANOVA). $^{\#}P < 0.01$; $^{\#\#}P < 0.001$. (**C**) Representative whole hearts, H&E-stained cross sections, and summary results for heart weight normalized to tibia length (HW/TL) in *Rgs2*$^{+/+}$ and *Rgs2*$^{-/-}$ hearts subjected to 1 wk TAC. White bar shows data from deceased mice. (**D**) Kaplan-Meier survival curve showing markedly increased mortality in *Rgs2*$^{-/-}$ mice subjected to TAC compared with littermate controls. (**E**) Wet lung weight normalized to body weight (n = 8–13 per group). White bar shows data from deceased mice. (**F**) Representative Masson's trichrome staining of the heart section. Blue stain indicates collagen deposition. Scale bars: 100 μm. Also shown are summary quantification results on myocyte diameter and collagen fraction (n = 4 hearts per group; >50 cells per heart; 5–6 sections for fibrosis analysis). $^{*}P < 0.05$ versus *Rgs2*$^{+/+}$ sham; $^{\S}P < 0.05$ versus *Rgs2*$^{-/-}$ sham; $^{\dagger}P < 0.05$ versus *Rgs2*$^{+/+}$ TAC.

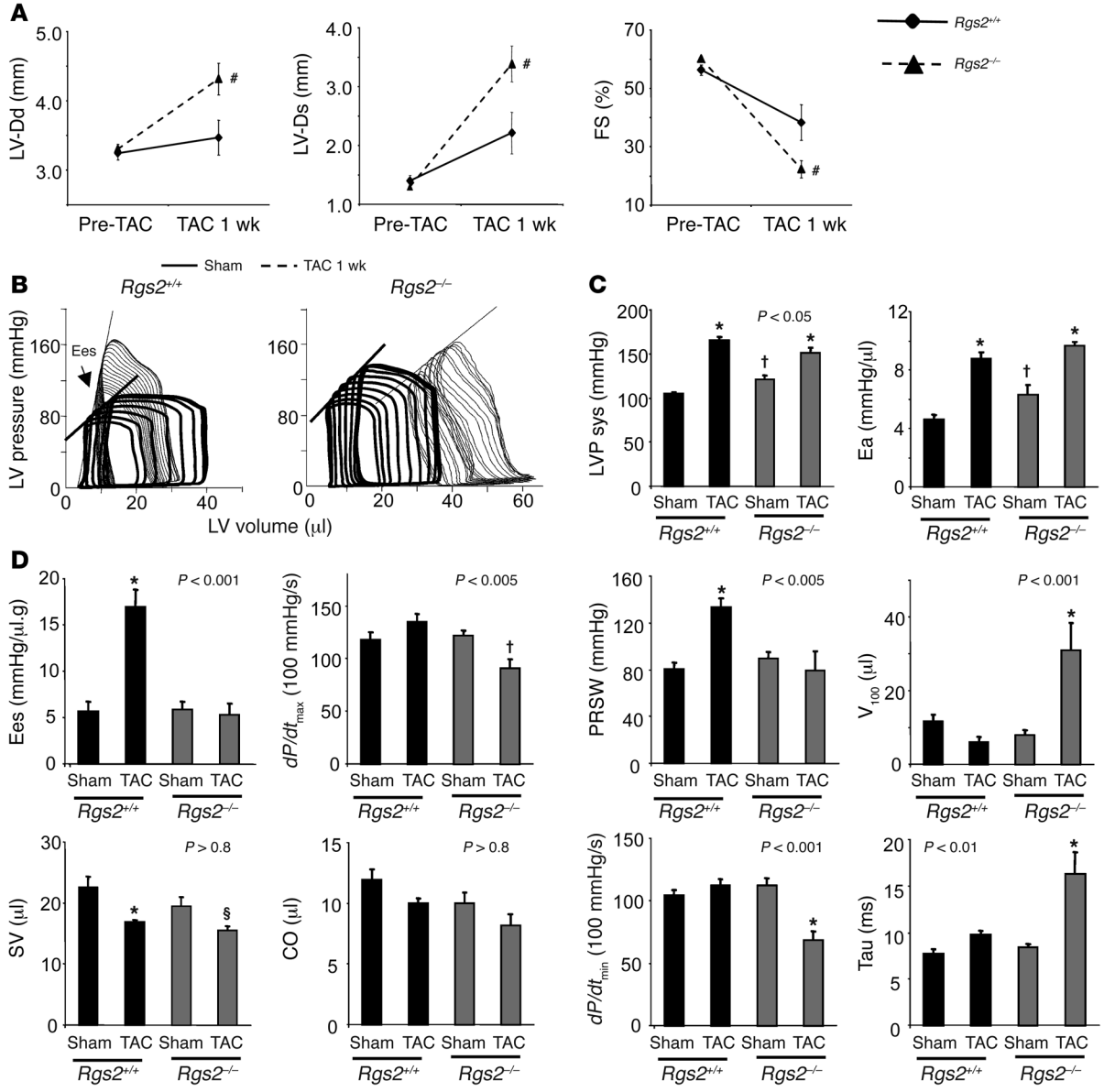

Figure 2

Rgs2$^{-/-}$ hearts display chamber dilation and fail to compensate to TAC. (**A**) Echocardiographic data before and after 1 wk TAC ($n = 7$ per group). LV-Dd, LV end-diastolic dimension; LV-Ds, LV end-systolic dimension. $^{\#}P < 0.05$ versus *Rgs2*$^{+/+}$ 1 wk TAC. (**B**) Representative PV loops during preload reduction by inferior vena cava occlusion in sham (thick line) and 1 wk TAC animals (thin dotted line). Steepness of left upper relation (end-systolic elastance [Ees]) reflected contractile function and was enhanced after TAC in *Rgs2*$^{+/+}$ mice, but unaltered with a right-shift (remodeling) of the relation in *Rgs2*$^{-/-}$ mice. (**C**) Peak systolic LV pressure (LVP sys) and effective arterial elastance (Ea; an index of total ventricular afterload). *Rgs2*$^{-/-}$ mice had somewhat higher basal afterload, but both genotypes had similarly increased afterload after 1 wk TAC ($n = 5$–7 per group). *P* value shown is for interaction of genotype and condition. $^{*}P < 0.05$ versus sham; $^{\dagger}P < 0.05$ versus *Rgs2*$^{+/+}$ sham. (**D**) Summary data obtained from PV loop analysis shown in bar graphs. *P* values shown are for interaction of genotype and condition (2-way ANOVA). $^{*}P \leq 0.001$, $^{\dagger}P < 0.05$ versus sham. V_{100}, volume position (end-systolic volume at common end-systolic pressure — 100 mmHg — derived from end-systolic PV relation); dP/dt_{max}, peak rate of LV pressure rise; PRSW, preload recruitable stroke work; dP/dt_{min}, peak rate of LV pressure decline; Tau, relaxation time constant; SV, stroke volume; CO, cardiac output. *P* values shown are for interaction of genotype and condition (2-way ANOVA). $^{*}P < 0.05$, $^{\S}P = 0.06$ versus sham; $^{\dagger}P < 0.05$ versus corresponding *Rgs2*$^{+/+}$ TAC and *Rgs2*$^{-/-}$ sham (1-way ANOVA).

Overexpression of $G_{\alpha q}$ itself lowered heart rate, as described previously (24), but this was not altered by deleting *Rgs2*.

Finally, we examined the cardiac response to a stress that did not involve G_q stimulation. *Rgs2*$^{-/-}$ and *Rgs2*$^{+/+}$ mice were subjected to 6 wk of swimming exercise (twice daily for 90 min). This regimen stimulated an increase in LV mass of about 30% in both groups, with no impairment of cardiac function (Figure 4F). Protein analysis confirmed that Cn, CaMKII, and ERK1/2 were not activated in either genotype by the exertional stress (Supplemental Figure 3). Thus, unlike our findings with TAC or

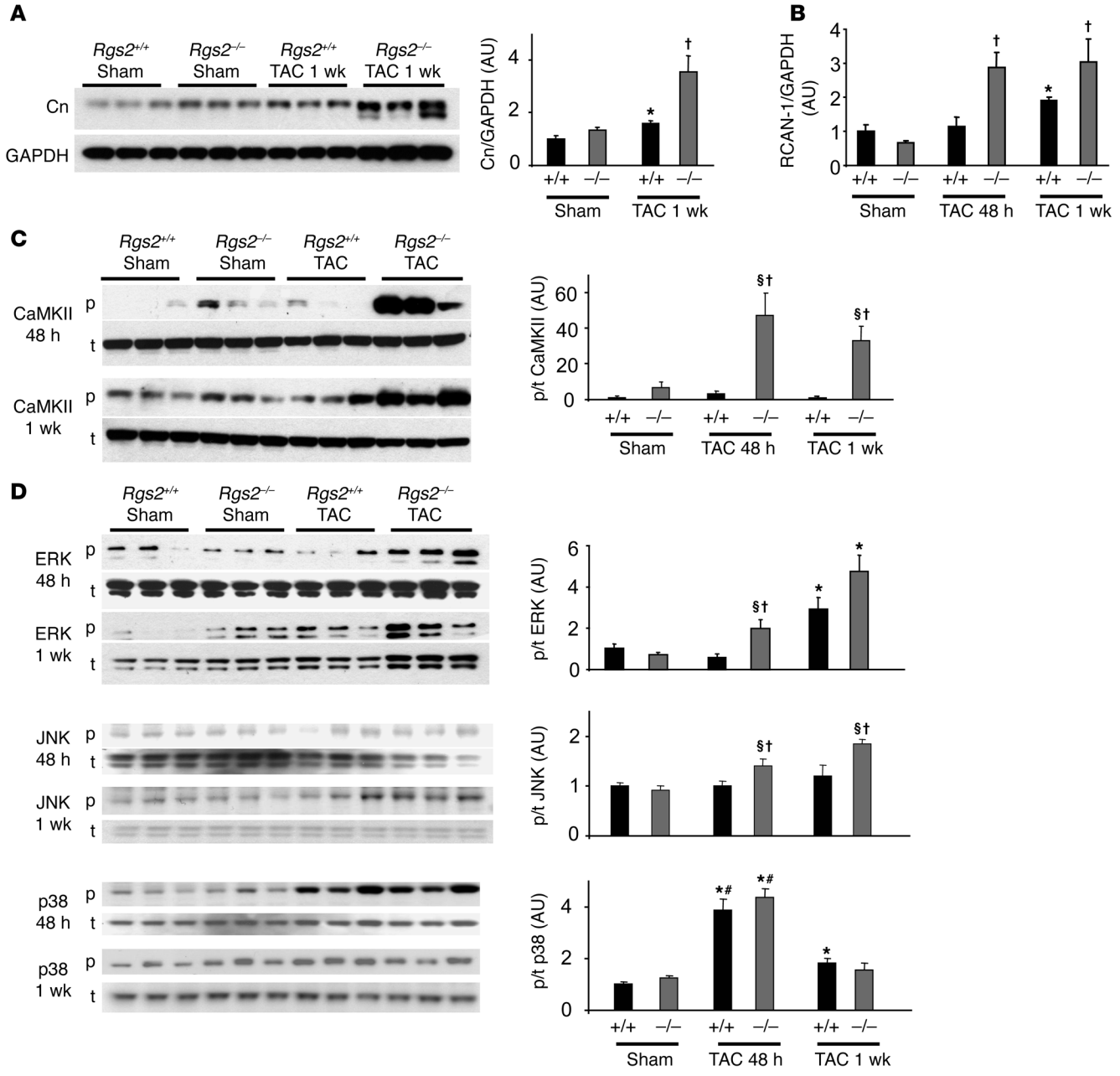

Figure 3

Robust early myocardial activation of G_q-related cascades after TAC in *Rgs2*$^{-/-}$ mice. (**A**) Immunoblot blot for Cn protein expression in 1 wk TAC and summary data normalized to GAPDH. (**B**) RCAN-1 mRNA expression (Cn activity) in hearts of mice subjected to 48 h and 1 wk TAC (n = 4–6 per group). (**C**) Phosphorylated (p; Thr286) and total (t) expression of CaMKII in hearts of mice subjected to 48 h and 1 wk TAC. Summary graph shows phosphorylated/total (p/t) CaMKII ratio. (**D**) Phosphorylated and total protein expression for MAPKs ERK1/2, JNK, and p38 assessed at baseline and after 48 h and 1 wk TAC. Summary bar graphs (n = 3–6 for each) show phosphorylated/total expression ratios for each kinase. *P < 0.05 versus respective sham; †P < 0.05 versus respective *Rgs2*$^{+/+}$ control; §P < 0.05 versus *Rgs2*$^{-/-}$ sham; #P < 0.05 versus respective 1 wk TAC.

$G_{\alpha q}$-OE$^+$ animals, hypertrophic response that did not involve G_q signaling stimulation was not exacerbated by a lack of RGS2.

Antihypertrophic effect of PDE5 inhibition is absent in Rgs2$^{-/-}$ *mouse hearts.* In noncardiac cells, RGS2 is activated by PKG-1α binding and phosphorylation, inducing their translocation to the outer plasma membrane to inactivate G_q (19). In hearts exposed to stress, cardiac PKG can be potently activated by inhibiting the cGMP hydrolytic enzyme PDE5, which in turn suppresses hypertrophy and/or dysfunction in mice subjected to pressure overload (21). While various individual PKG targets may underlie this response (25), RGS2 could reflect a very proximal effecter that subsequently regulates multiple downstream cascades. To test the importance of RGS2 to this regulation, mice were fed with the PDE5 inhibitor sildenafil during 1 wk TAC. Sildenafil blunted hypertrophy in controls, reducing wall thickness and chamber size and improving FS, but had no effect on these properties in *Rgs2*$^{-/-}$ TAC hearts (Figure 5, A–C).

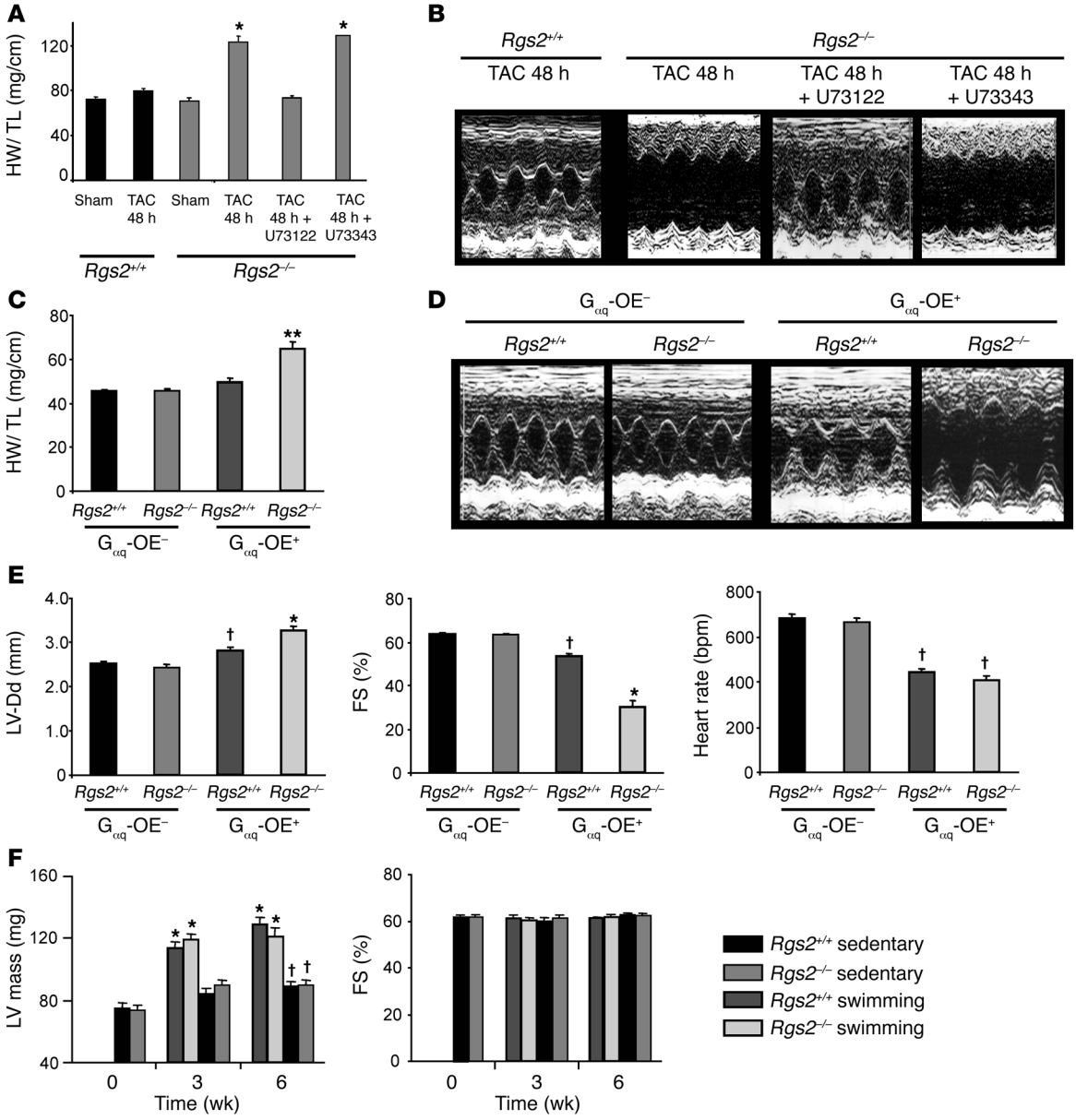

Figure 4

$G_{\alpha q}$ as a critical target of RGS2. (**A**) Inhibition of PLCβ with U73122 prevents exacerbated hypertrophy (heart weight/tibia length), chamber dilation, and dysfunction (n = 7–14 per group). *P < 0.001 versus other groups. (**B**) In *Rgs2*$^{-/-}$ mice subjected to 48 h TAC, the inactive control agent U73343 did not suppress pathological remodeling. Summary echo data are provided in Supplemental Figure 2B. (**C**) Cardiac hypertrophy was exacerbated in double-mutant $G_{\alpha q}$-OE^{+}*Rgs2*$^{-/-}$ mice (n = 7–9 per group). **P < 0.01 versus other groups. (**D**) Corresponding echocardiograms showed worsened function and chamber dilation. (**E**) Summary data for LV diastolic dimension, FS, and heart rate (n = 7–9 per group). *P < 0.05 versus other groups; †P < 0.05 versus all $G_{\alpha q}$-OE^{-} groups. (**F**) Response of cardiac LV mass and echocardiographic FS in mice subjected to swimming versus sedentary animals. Exercise-induced hypertrophy was similar in *Rgs2*$^{+/+}$ and *Rgs2*$^{-/-}$ mice, with no change in FS. *P < 0.01, †P < 0.05 versus respective week-0 baseline.

Sildenafil also improved contractility and relaxation in *Rgs2*$^{+/+}$ mice exposed to TAC, which was not observed in *Rgs2*$^{-/-}$ mice (Figure 5, D and F). As previously reported (21), sildenafil did not itself reduce cardiac afterload (Figure 5E).

Because *Rgs2*$^{-/-}$ mice displayed greater activation of G_q-linked pathways (Cn, CaMKII, and ERK1/2), we tested whether sildenafil suppresses these signaling pathways in *Rgs2*$^{+/+}$ and *Rgs2*$^{-/-}$ hearts. Activation of each enzyme was indeed blunted by sildenafil cotreatment in *Rgs2*$^{+/+}$ TAC hearts, an effect not observed in *Rgs2*$^{-/-}$ TAC hearts (Figure 6, A–C).

Regulation of RGS2 by PKG-1α. Because PKG interacts with proteins other than RGS2, the absence of PDE5 inhibition effects in *Rgs2*$^{-/-}$ mice raised the question of whether PKG activation had in fact occurred in these hearts. Baseline PKG activity was not significantly different between models (P = 0.2), and importantly, both displayed similar relative increases in activity after 1 wk TAC and

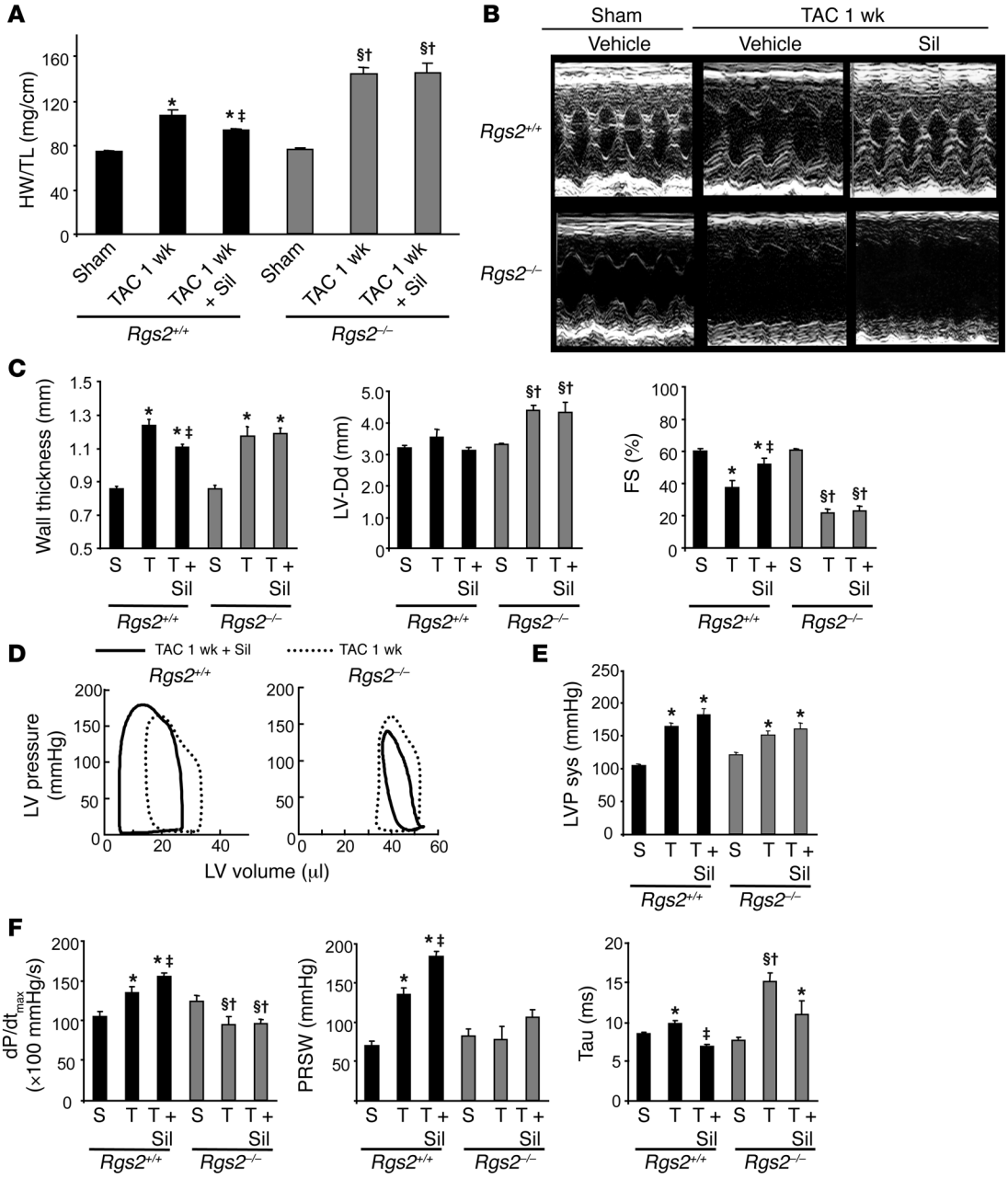

Figure 5

Amelioration of pressure load–induced cardiac hypertrophy/remodeling via PDE5 inhibition with sildenafil is absent in *Rgs2*$^{-/-}$ mice. (**A**) Sildenafil (Sil) suppressed hypertrophy in *Rgs2*$^{+/+}$, but not *Rgs2*$^{-/-}$, mice (n = 8–13 per group). (**B** and **C**) Representative echocardiograms and summary data showing response to 1 wk TAC (T) with or without sildenafil treatment (n = 7–9 per group). S, sham. (**D**) Effects of sildenafil on LV PV loops. (**E**) Sildenafil did not alter the increase in LV afterload in either genotype (n = 4–7 per group). (**F**) Summary invasive PV loop results (n = 4–7 per group). Sildenafil improved systolic and diastolic function in *Rgs2*$^{+/+}$ TAC hearts, but had no effect in *Rgs2*$^{-/-}$ TAC hearts. *P < 0.05 versus respective sham control; ‡P < 0.05 versus respective 1 wk TAC; †P < 0.05 versus *Rgs2*$^{+/+}$ TAC; §P < 0.05 versus *Rgs2*$^{-/-}$ sham.

substantial further enhancement with sildenafil treatment (Figure 7A; P = 0.37, genotype and genotype × condition; P < 0.0001, condition effect; 2-way ANOVA). Thus, the lack of a sildenafil effect in *Rgs2*$^{-/-}$ could not be attributed to lack of PKG activation per se.

PKG-1α activates RGS2 in vascular smooth muscle (19), leading to translocation of both proteins to the outer cell membrane; furthermore, PKG-1α is the prominent isoform in the heart (25). Therefore, we examined the localization of both proteins in cardiac myocytes. In control cells, RGS2 displayed faint diffuse cytosolic and membrane localization, whereas PKG-1α was diffusely distributed with a somewhat striated pattern (Figure 7B). After 2 h exposure to the G_q agonist ET1, both RGS2 and PKG-1α intensified at the outer membrane (Figure 7B). Identical results were obtained using angiotensin II stimulation (data not shown). This translocation was fully blocked by coincubation with the specific PKG peptide inhibitor DT2 (26) and was conversely stimulated by 8Br-cGMP

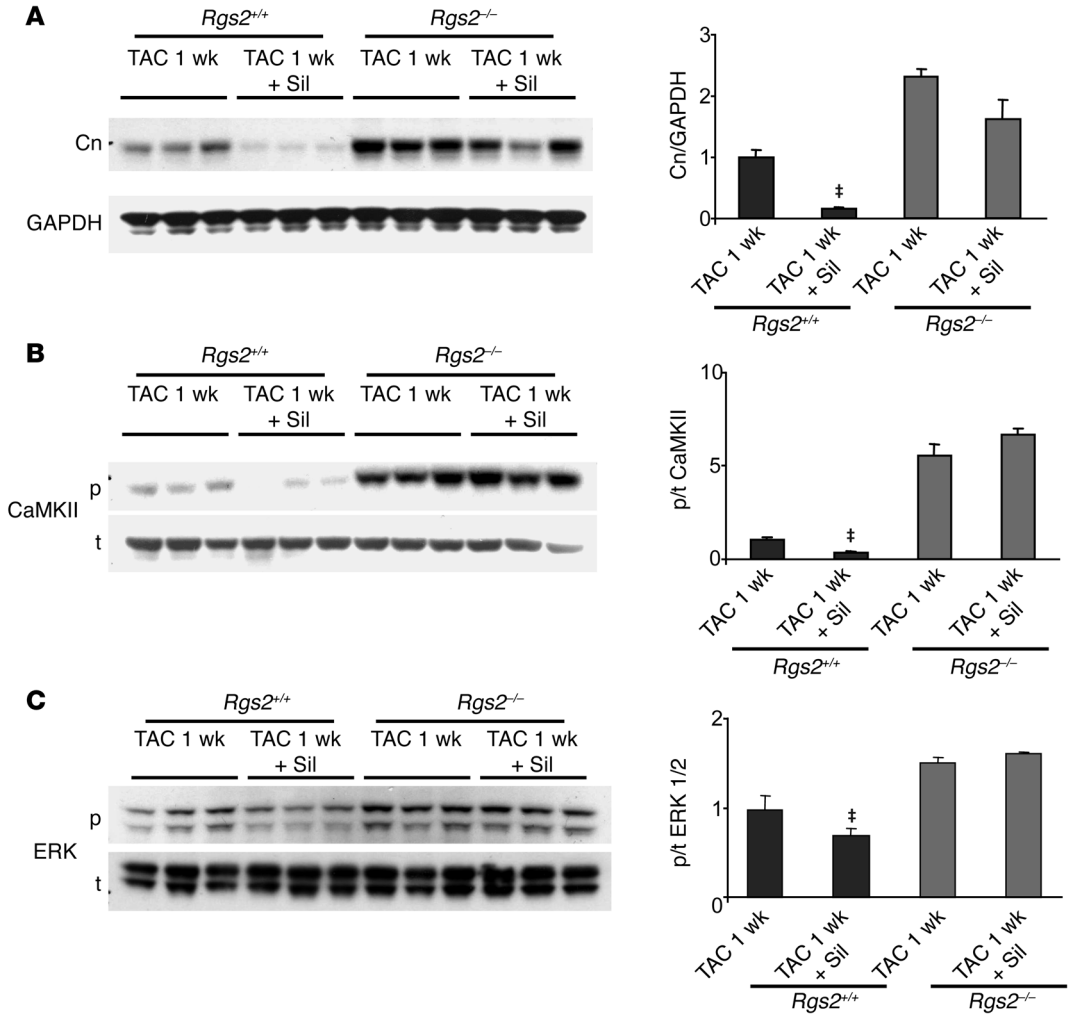

Figure 6
Sildenafil suppresses $G_{\alpha q}$-coupled molecular cascades in *Rgs2*$^{+/+}$, but not *Rgs2*$^{-/-}$, hearts. (**A**) Protein expression for Cn. (**B** and **C**) Phosphorylated and total protein expression for CaMKII (**B**) and ERK1/2 (**C**). Summary data are shown for each (n = 3–6 per group). ‡$P < 0.05$ versus *Rgs2*$^{+/+}$ 1 wk TAC.

(Figure 7B). Importantly, translocation of both proteins was also observed after TAC in *Rgs2*$^{+/+}$ hearts, evident at 48 h and declining by 1 wk. Sildenafil treatment enhanced membrane localization of both proteins after 1 wk TAC, consistent with enhanced PKG activity. In *Rgs2*$^{-/-}$ cells, basal PKG-1α localization was similar to *Rgs2*$^{+/+}$ cells (Supplemental Figure 4A). Intriguingly, PKG-1α also translocated to the outer membrane after 48 h TAC; however, this was mostly absent by 1 wk TAC (Figure 7C). Moreover, unlike controls, concomitant inhibition of PDE5 did not significantly alter this localization. These confocal results were confirmed by cell-fraction protein immunoblots (Figure 7D; gel loading data provided in Supplemental Figure 4B).

Discussion

The present study demonstrates a major cardiac regulatory role for RGS2 as a critical brake against the $G_{\alpha q}$/PLCβ pathway in the early cardiac stress response to pressure overload. Without RGS2, pressure overload induced rapidly exacerbated hypertrophy and dysfunction, amplified G_q-coupled signaling, and early mortality. Deletion of *Rgs2* in $G_{\alpha q}$ transgenic hearts worsened dilation and hypertrophy, whereas inhibiting PLCβ blocked the rapid deterioration and hypertrophy after TAC in *Rgs2*$^{-/-}$ hearts. Swimming, a non–G_{aq}-coupled stress (1, 27), had no adverse effect in these mice. Finally, we showed that the capacity of cGMP/PKG stimulated by PDE5 inhibition to blunt hypertrophy and enhance cardiac function within the first week of pressure overload stress was critically coupled to RGS2 and its suppression of G_q signaling.

Rgs2$^{-/-}$ mice exhibited a very rapid hypertrophic response to pressure overload, revealing both the early potency of G_q stimulation and a key role of its suppression by RGS2 to permit early compensation. This finding demonstrates that the transition from adaptive to maladaptive hypertrophy involves not only the magnitude and duration of proremodeling stimuli, but also the robustness and sustainability of critical countermeasures that blunt their toxicity. Stimulation of G_q by TAC can reflect both receptor/agonist interaction from neurohormones and mechanical stretch, as described previously via the angiotensin II receptor (28, 29). The *Rgs2*$^{-/-}$ phenotype is somewhat unusual in that animals have

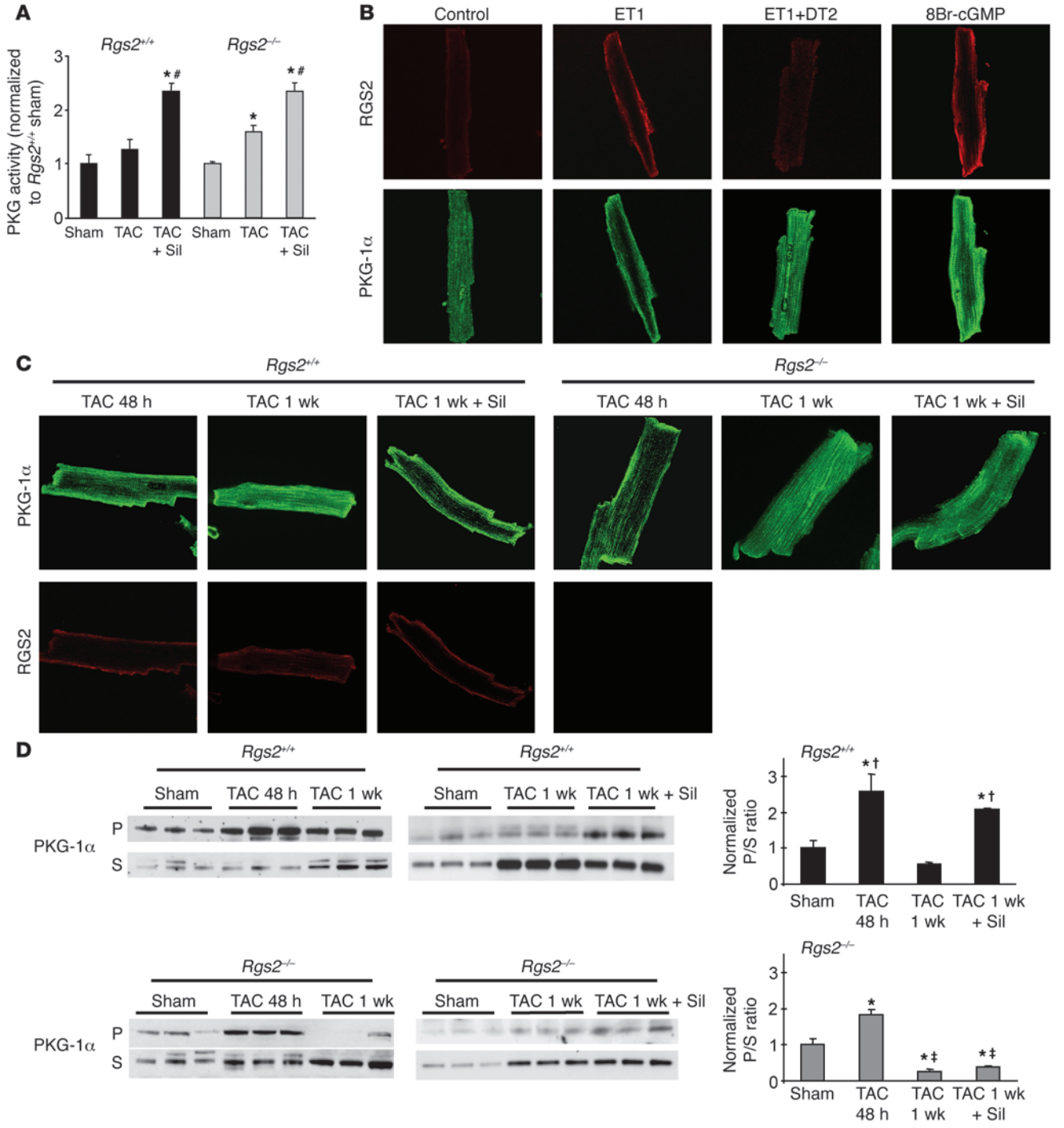

Figure 7

Regulation of RGS2 by PKG-1α. (**A**) PKG is similarly activated with and without concomitant sildenafil treatment in both genotypes. *$P < 0.05$ versus respective sham; #$P < 0.005$ versus TAC alone. (**B**) Subcellular localization of RGS2 and PKG-1α in *Rgs2*$^{+/+}$ mouse adult cardiac myocytes by immunohistochemistry using confocal microscope. Images represent baseline (control), ET1 stimulation, ET1 stimulation with PKG inhibitor (ET1+DT2), and PKG stimulation with 8Br-cGMP. More than 20 cells were analyzed from 1 experiment, and experiments were repeated 3 times. Original magnification, ×200. (**C**) Translocation of PKG-1α to outer membrane with 48 h TAC occurred in both genotypes and declined somewhat after 1 wk in *Rgs2*$^{+/+}$ mice but was virtually absent in *Rgs2*$^{-/-}$ mice at the same time. Sildenafil treatment restored membrane localization and enhanced RGS2 membrane signal in *Rgs2*$^{+/+}$ cells, but had no impact in *Rgs2*$^{-/-}$ cells. Original magnification, ×200. (**D**) Immunoblot of PKG-1α from cytosolic (soluble [S]) and membrane (particulate [P]) fractions in sham control, 48 h, and 1 wk TAC myocardium. Summary data of particulate/soluble ratio is shown at right (n = 3–6 per group). *$P < 0.001$ versus sham; †$P < 0.001$ versus 1 wk TAC; ‡$P < 0.001$ versus 48 h TAC. Equal protein loading was confirmed by Ponceau staining (Supplemental Figure 4B).

normal heart function and LV mass at rest, yet develop marked hypertrophy, dilation, and early mortality after TAC. Genetic models lacking cardiac protective or structural genes that exhibit early mortality after TAC (e.g., gp130 and integrin β_1–interacting protein; refs. 30, 31) dilate without hypertrophy, whereas others (e.g., dominant-negative thioredoxin-1 and inactivated glycogen synthase kinase–3β; refs. 32, 33) induce hypertrophy that worsens further with TAC, yet do not display early lethality.

Other RGS proteins, such as RGS3 and RGS4, may also be involved in hypertrophy and failure regulation (10, 34), although these proteins are less specific to G_q (6). Mice with myocyte-targeted RGS4 overexpression exhibit a complex phenotype, developing rapid dilation and early mortality (1–2 days) without hypertrophy after exposure to TAC, but survivors exhibit less eventual hypertrophy (11). When these animals are genetically crossed with $G_{\alpha q}$-OE$^+$ mice, cardiac abnormalities in the latter strain are ameliorated (9). Thus, RGS4 may have protective roles in the later stages of disease, consistent with its upregulation in end-stage human heart failure (7, 35). RGS4 may also mediate ameliorative effects of natriuretic peptides on cardiac stress remodeling, although in vivo support for this hypothesis is so far based on the ability of RGS4 overexpression to blunt the cardiac phenotype in mice genetically lacking natriuretic peptide receptor–coupled guanylate cyclase–A (10).

RGS2 modulates stress response signaling by several mechanisms (36, 37). First, it inactivates the $G_{\alpha q}$ subunit, which can suppress downstream Ca^{2+}-activated cascades (including Cn and CaMKII) and MAPKs (including ERK and JNK), as shown in the current study. Cn and CaMKII in particular are considered potent contributors to maladaptive remodeling (22, 38). The results of the present studies using PLCβ inhibition, genetic deletion of *Rgs2* in $G_{\alpha q}$-OE$^+$ mice, and swimming exercise support RGS2 suppression of $G_{\alpha q}$/PLCβ signaling as a central feature of its cardioprotective effects. RGS proteins can also inhibit $G_{\beta\gamma}$-induced signaling by reforming the G protein heterotrimer, and this could influence Akt/glycogen synthase kinase–3β cascades (39), which we have previously shown to be suppressed by PDE5 inhibition (21). RGS proteins can further bind to effecter enzymes, such as adenylate cyclase and PKC isoforms, to blunt signaling (40), although the role of this modulation in heart remains unknown.

While RGS2 has high affinity for G_q, it can suppress $G_{i/o}$ or G_s in some cell types. For example, it regulates presynaptic Ca^{2+} channels via $G_{\beta\gamma}$ subunits in neurons (41) and impacts carbachol-stimulated activation of ERK and Akt in COS cells via $G_{i/o}$ interaction (42). RGS2 blunts G_s-coupled cAMP accumulation triggered by parathyroid hormone–related peptide (43). However, the effects of RGS2 over $G_{i/o}$ or G_s appear to be unimportant in adult cardiac myocytes, as neither muscarinergic nor β-adrenergic cAMP regulation is altered by RGS2 overexpression in contrast to RGS3, RGS4, or RGS5 (6).

Even though PDE5 is more abundantly expressed in vascular smooth muscle, antihypertrophic effects from its inhibition are likely caused by direct cardiac effects. First, as demonstrated in the present study, cardiac afterload associated with TAC was unchanged by sildenafil treatment. Second, PDE5 inhibition suppresses Cn/nuclear factor of activated T cell (Cn/NFAT) signaling and expression of the genes encoding atrial and brain natriuretic peptides in isolated myocytes stimulated with a G_q agonist (21, 44). Third, knockdown of the gene encoding PDE5 in cardiac myocytes is antihypertrophic, having an impact similar to that of sildenafil, and the effect of combining both is similar to that of each alone (44). This last finding supports specificity of sildenafil for inhibiting PDE5. The improvement in cardiac function by sildenafil involves several mechanisms, including enhanced myocyte calcium cycling and a decline in PKCα activation (45), both potentially linked to RGS2 suppression of $G_{\alpha q}$/PLCβ.

Growing evidence supports an important role for myocardial cGMP/PKG signaling as an intrinsic brake to suppress maladaptive cardiac stress remodeling (46); however, only recently have studies revealed potential mechanisms for this effect. The first reported target was Cn/NFAT, which can be suppressed in neonatal myocytes by enhancing cGMP (e.g., NO donors) or expressing activated PKG (47). PDE5 inhibition was shown to have a similar effect in vivo (21), and our present data further support this. PKG also blunts RhoA activation by phosphorylation at Ser188 (48), although whether this applies to myocytes remains unknown. PKG phosphorylates SMAD3 at Ser309 and Thr388 in fibroblasts, preventing its nuclear translocation to block TGF-β1 activation (49). This may be important for how PDE5 inhibitors suppress fibrosis. PKG can also block p38 autophosphorylation coupled to its binding to the scaffold protein TGF-β–activated protein kinase 1–binding protein 1 (TAB1) in ischemia/reperfusion injury (50), although this mechanism does not appear to be involved in 1 wk TAC. While the latter pathways involve direct PKG phosphorylation, similar mechanisms have not been identified for Cn/NFAT or CaMKII suppression. However, as these enzymes are coupled to G_q stimulation, suppression of the proximal signal by RGS2-PKG activation could provide a mechanism as well as explain reduced RhoA and TGF-β stimulation.

In vascular smooth muscle cells, activation of RGS2 by the nitric oxide/cGMP pathway requires binding to PKG-1α and its phosphorylation at Ser46 and Ser64 by PKG-1α, but RGS2 does not need the G_q-coupled pathway to be activated (19). cGMP stimulation also increases the association of the smooth muscle cell plasma membrane with wild-type but not mutant (S46,64A) RGS2 (51), highlighting the importance of PKG activity for this association and GPCR modulation. The current study is the first to our knowledge to show that PKG-1α rapidly translocates to the outer plasma membrane from a resting cytosolic distribution in adult mouse myocytes in vitro and in vivo, concurrent with RGS2 plasma membrane localization, and that PKG activation is required for this movement. The acute movement of PKG-1α to the plasma membrane even in *Rgs2*$^{-/-}$ cells indicates that another chaperone is involved, if not more than one. This may require binding to the leucine zipper motif in PKG-1α, as deletion of this motif in PKG-1β — the other isoform harboring the only difference at leucine zipper motif — translocates the enzyme to the nucleus upon activation in BHK cells (52). Importantly, PKG-1α translocation was more transient in *Rgs2*$^{-/-}$ myocytes than in controls and did not provide antihypertrophic protection. *Rgs2*$^{-/-}$ TAC hearts showed relative PKG activation by 1 wk sildenafil treatment similar to that of *Rgs2*$^{+/+}$ hearts; thus, compartmentalization of this signal and its specific interaction with RGS2 appears to be central to its capacity to suppress G_q signaling and maladaptive hypertrophy.

Our study has several limitations. The *Rgs2*$^{-/-}$ mice globally lacked the gene, and though cardiac function was unchanged (observed even in 10-month-old animals; Supplemental Table 3), adaptive responses to sustained modest hypertension could still occur. Although there were no basal differences in the signaling cascades examined, our analysis was admittedly quite focused. Importantly, TAC-induced pressure overload was similar in both genotypes, and whatever adaptations may have existed, they failed

to compensate to the higher afterload. The blood pressure disparity we observed was somewhat less than originally reported (17), yet similar to other studies using the same mouse model (53). Some of this disparity may relate to the anesthesia used in our protocol. Because the gene was absent from conception, we cannot yet assess the role of RGS2 in the later stages of pressure overload disease. Such assessment will require an inducible gene deletion model currently under development. However, our present results indicate that a dominating PKG effecter in the initial response to pressure overload is RGS2.

In summary, our study demonstrates an essential role for RGS2 — inhibiting the $G_{\alpha q}$/PLCβ pathway — in early compensatory hypertrophy development to pressure overload and provides a mechanism for antihypertrophic effects associated with PKG enhancement from PDE5 inhibition. This coactivation provides what we believe to be the most proximal target for PKG-mediated inactivation of hypertrophy stimulation thus far described and can explain how multiple distal pathways can be concomitantly suppressed by PDE5 inhibition.

Methods

Animal models. *Rgs2*$^{-/-}$ mice, which harbor a global RGS2 deletion, and *Rgs2*$^{+/+}$ littermate controls in C57BL/6 background were as reported previously (19), originally developed by J. Penninger (54). $G_{\alpha q}$-OE^{+} mice (40 copies of the transgene, FVB background; ref. 24), generously provided by G. Dorn (Washington University Center for Pharmacogenomics, St. Louis, Missouri, USA), were crossed with *Rgs2*$^{-/-}$ animals to generate animals lacking *Rgs2* and overexpressing $G_{\alpha q}$ in the heart. The same generation of animals ($G_{\alpha q}$-OE^{-}*Rgs2*$^{+/+}$, $G_{\alpha q}$-OE^{+}*Rgs2*$^{+/+}$, $G_{\alpha q}$-OE^{-}*Rgs2*$^{-/-}$, $G_{\alpha q}$-OE^{+}*Rgs2*$^{+/+}$) was also studied.

TAC. Pressure overload was produced by TAC in male *Rgs2*$^{-/-}$ and *Rgs2*$^{+/+}$ animals of 4–5 months of age (mean BW, 26 g) as previously described (21). Briefly, animals were anesthetized with isoflurane (2%–3%), intubated, and mechanically ventilated. The transverse aorta was constricted with a 26-gauge needle using 7-0 prolene suture, after which the chest was closed and the animal was allowed to recover from anesthesia. Control mice were subjected to sham operations, and animals were studied 48 h to 1 wk after surgery. Sets of male *Rgs2*$^{-/-}$ animals were subjected to 48 h TAC and treated daily with 2.5 mg/kg/d U73122, a specific PLCβ inhibitor, or U73343, its inactive analog, in peanut oil via i.p. injection. Additional animals in either genotype were subjected to 1 wk TAC while cotreated with sildenafil (200 mg/kg/d) mixed in food (Bioserve soft diet).

Swimming exercise. Male *Rgs2*$^{-/-}$ and *Rgs2*$^{+/+}$ animals (3 months of age; 23–25 g BW) were studied. The forced swimming program was a modified 6-wk protocol based on a prior method (55). Control animals remained sedentary in a cage for 6 wk. Briefly, 10 mice at a time swam twice daily in a 45-cm by 75-cm container with the water kept at approximately 32°C. Sessions began at 10 min and were increased by 10-min increments each day until each session lasted 90 min; this was then maintained for the remainder of the 6-wk period. Constant monitoring ensured the safety of the mice and prevented them from floating or holding their breath under water. All animal protocols were approved by the Animal Care and Use Committee of Johns Hopkins University.

Echocardiography. In vivo cardiac morphology was assessed by transthoracic echocardiography (Acuson Sequoia C256, 13-MHz transducer; Siemens) in conscious mice (21). M-mode LV end-systolic and end-diastolic dimensions were averaged from 3–5 beats. LV percent FS and LV mass were calculated as described previously (21). Wall thickness of lateral free wall and intraventricular septum were averaged. Studies and analysis were performed by investigators blinded to genotype or heart condition.

In vivo hemodynamics. In vivo LV function was assessed by PV catheter as described previously (21). Briefly, mice were anesthetized with 1%–2% isoflurane, 750–100 mg/kg urethane i.p., 5–10 mg/kg etomidate i.p., and 1–2 mg/kg morphine i.p.; were subjected to tracheostomy; and were ventilated with 6–7 μl/g tidal volume and 130 breaths/min. Volume expansion (12.5% human albumin, 50–100 μl over 5 min) was provided through a 30-gauge cannula via the right external jugular vein. The LV apex was exposed through an incision between the seventh and eighth ribs, and a 1.4-Fr PV catheter (SPR 839; Millar Instruments Inc.) was advanced through the apex to lie along the longitudinal axis. Absolute volume was calibrated, and PV data were measured at steady state and during transient reduction of venous return by occluding the inferior vena cava with a 6-0 silk snare suture. Data were digitized at 2 kHz, stored to disk, and analyzed with custom software. From the 10–15 successive cardiac cycles during the inferior vena cava occlusion, the end-systolic PV relation slope (i.e., end-systolic elastance) and stroke work–end-diastolic volume relation (i.e., preload recruitable stroke work) were derived.

Tissue histology. Myocardium fixed with 10% formalin was analyzed for myocyte hypertrophy and fibrosis. Tissue was paraffin embedded, cross-sectioned into 5- to 8-μm slices, and stained with H&E or Masson's trichrome staining (21). We analyzed 6 serial sections of mid-LV per heart. To assess mean cardiomyocyte diameter and interstitial collagen fraction, 6–8 regions of photomicrographs covering the whole section were obtained and quantified using computer-assisted image analysis (Adobe Photoshop version 5.0 and NIH Image J). Average data reflect results from 4–5 hearts per group (>50 cells).

Western blot analysis. Protein was prepared from snap-frozen heart tissue or isolated cardiac myocytes, and fractionation was performed as previously described (21, 56). After homogenization in 25 mM Tris-HCL, pH 7.5, 4 mM EGTA, 2 mM EDTA, 5 mM dithiothreitol, 1 mM phenylmethylsulfonyl fluoride, and 1 μM leupeptin and incubation on ice for 30 min, samples were spun at 100,000 *g* for 30 min at 4°C. The supernatant was saved as the cytosolic fraction, and the pellet was resuspended in homogenization buffer with 1% Triton X-100 added. This was processed as described previously (56), and the remaining supernatant was saved as the particulate fraction. Protein concentration was measured by BCA assay (Pierce Biotechnology). Protein extracts were run on 4%–12% Bis-Tris NuPage gels (Invitrogen), blotted onto nitrocellulose membranes, and probed with the following primary antibodies: rabbit polyclonal antibody generated against synthesized peptide KKPQITTEPHAT corresponding to RGS2 C terminus; Cn (diluted 1:500; BD Biosciences; ref. 21); Thr286–phospho-CaMKII (diluted 1:1,000; Affinity BioReagents); ERK, Thr202/Thr204–phospho-ERK, JNK, Thr183/Tyr185–phospho-JNK, p38, and Thr180/Tyr182-p38 (diluted 1:1,000; Cell Signaling Technology; ref. 21); PKG-1α (diluted 1:1,000); and GAPDH (diluted 1:3,000; IMGENEX or Cell Signaling Technology). Antibody binding was visualized by horseradish peroxidase–conjugated secondary antibodies and enhanced chemiluminescence (Pierce Biotechnology).

Quantitative real-time PCR. Total RNA was extracted from snap-frozen heart tissue using TRIzol reagent (Invitrogen; ref. 21). The yield and purity of RNA was estimated spectrophotometrically using A260/A280 ratio. RNA (1 μg) was reverse transcribed into cDNA using SuperScript first-strand synthesis system (Invitrogen). cDNA was subjected to PCR amplification using TaqMan PCR Master Mix reagent (Applied Biosystems). TaqMan primers and probes for *Rgs2*, *Nppa*, *Nppb*, *Myh7*, *Atp2a2*, *Rcan1*, *18S*, and *Gapdh* were purchased from Applied Biosystems.

Adult mouse myocyte preparation and immunohistochemistry. Mouse adult ventricular myocytes were isolated, fixed, and stained for confocal immunohistochemistry as described previously (57). Cells were plated on laminin-coated 6-well dishes in medium, and incubated in Tyrode's solution with angiotensin (1 μM for 2 h; Sigma-Aldrich) or ET1 (0.5 μM for 2 h; Sigma-Aldrich) in the presence or absence of DT2 compound

(5 μM; Biolog; ref. 26) or 8Br-cGMP (1 mM for 1 h; Sigma-Aldrich; ref. 19). Cells were fixed with 50% methanol and 50% acetone, permeabilized with 0.1% saponin in PBS, blocked in 10% BSA in PBS, incubated overnight with primary antibodies at 4°C (goat anti-RGS2, diluted 1:100; Santa Cruz Biotechnology Inc.; rabbit anti–PKG-1α, diluted 1:400), and subsequently incubated with secondary antibodies for 1 h at room temperature (Alexa Fluor 546–conjugated donkey anti-goat and Alexa Fluor 488–conjugated donkey anti-rabbit; Invitrogen). Imaging was performed on a Zeiss inverted epifluorescent microscope (Carl Zeiss Inc.) attached to an argon-krypton laser confocal scanning microscope (UltraView; Perkin Elmer Life Science Inc.).

Protein synthesis of adult mouse cardiac myocytes. Protein synthesis was measured by [^{3}H] leucine incorporation. After overnight culture, cells were stimulated with 100 nM ET1. After ET1 stimulation, [^{3}H] leucine (1 μCi/ml) was add to the culture medium, and cells were further incubated for 24 h. The incorporated [^{3}H] leucine was measured using a liquid-scintillation counter.

Statistics. All values are expressed as mean ± SEM. Group data were compared using 1- or 2-way ANOVA (with genotype and sham or TAC as categories) and Tukey's post-hoc multiple-comparisons test for between-group differences. Comparisons between 2 groups were made using nonpaired 2-tailed Student's *t* test. A *P* value less than 0.05 was considered significant. Sample sizes and individual statistical results for all analyses are provided in the figures, supplemental figures, and supplemental tables.

Acknowledgments

This work was supported by American Heart Association SDG 630026N (E. Takimoto), by a fellowship grant from Daiichi-Sankyo (T. Nagayama), and by National Heart, Lung, and Blood Institute grants HL-089297, HL-077180, HL-084986, and HL-59408 (D.A. Kass). The authors thank Gerald Dorn for generously providing the $G_{\alpha q}$-OE$^+$ mice.

Received for publication March 14, 2008, and accepted in revised form November 12, 2008.

Address correspondence to: Eiki Takimoto or David A. Kass, Ross 858, Division of Cardiology, Department of Medicine, Johns Hopkins University Medical Institutions, 720 Rutland Avenue, Baltimore, Maryland 21205, USA. Phone: (410) 955-7153; Fax: (410) 502-2558; E-mail: etakimo1@jhmi.edu (E. Takimoto); dkass@jhmi.edu (D.A. Kass).

1. Dorn, G.W., and Force, T. 2005. Protein kinase cascades in the regulation of cardiac hypertrophy. *J. Clin. Invest.* **115**:527–537.
2. Heineke, J., and Molkentin, J.D. 2006. Regulation of cardiac hypertrophy by intracellular signalling pathways. *Nat. Rev. Mol. Cell Biol.* **7**:589–600.
3. Wieland, T., Lutz, S., and Chidiac, P. 2007. Regulators of G protein signalling: a spotlight on emerging functions in the cardiovascular system. *Curr. Opin. Pharmacol.* **7**:201–207.
4. Abramow-Newerly, M., Roy, A.A., Nunn, C., and Chidiac, P. 2006. RGS proteins have a signalling complex: interactions between RGS proteins and GPCRs, effectors, and auxiliary proteins. *Cell Signal.* **18**:579–591.
5. Riddle, E.L., Schwartzman, R.A., Bond, M., and Insel, P.A. 2005. Multi-tasking RGS proteins in the heart: the next therapeutic target? *Circ. Res.* **96**:401–411.
6. Hao, J., et al. 2006. Regulation of cardiomyocyte signaling by RGS proteins: differential selectivity towards G proteins and susceptibility to regulation. *J. Mol. Cell. Cardiol.* **41**:51–61.
7. Mittmann, C., et al. 2002. Expression of ten RGS proteins in human myocardium: functional characterization of an upregulation of RGS4 in heart failure. *Cardiovasc. Res.* **55**:778–786.
8. Tamirisa, P., Blumer, K.J., and Muslin, A.J. 1999. RGS4 inhibits G-protein signaling in cardiomyocytes. *Circulation.* **99**:441–447.
9. Rogers, J.H., et al. 2001. RGS4 reduces contractile dysfunction and hypertrophic gene induction in Galpha q overexpressing mice. *J. Mol. Cell. Cardiol.* **33**:209–218.
10. Tokudome, T., et al. 2008. Regulator of G-protein signaling subtype 4 mediates antihypertrophic effect of locally secreted natriuretic peptides in the heart. *Circulation.* **117**:2329–2339.
11. Rogers, J.H., et al. 1999. RGS4 causes increased mortality and reduced cardiac hypertrophy in response to pressure overload. *J. Clin. Invest.* **104**:567–576.
12. Cifelli, C., et al. 2008. RGS4 regulates parasympathetic signaling and heart rate control in the sinoatrial node. *Circ. Res.* **103**:527–535.
13. Cavalli, A., Druey, K.M., and Milligan, G. 2000. The regulator of G protein signaling RGS4 selectively enhances alpha 2A-adreoreceptor stimulation of the GTPase activity of Go1alpha and Gi2alpha. *J. Biol. Chem.* **275**:23693–23699.
14. Heximer, S.P., Watson, N., Linder, M.E., Blumer, K.J., and Hepler, J.R. 1997. RGS2/G0S8 is a selective inhibitor of Gqalpha function. *Proc. Natl. Acad. Sci. U. S. A.* **94**:14389–14393.
15. Akhter, S.A., et al. 1998. Targeting the receptor-Gq interface to inhibit in vivo pressure overload myocardial hypertrophy. *Science.* **280**:574–577.
16. Wettschureck, N., et al. 2001. Absence of pressure overload induced myocardial hypertrophy after conditional inactivation of Galphaq/Galpha11 in cardiomyocytes. *Nat. Med.* **7**:1236–1240.
17. Heximer, S.P., et al. 2003. Hypertension and prolonged vasoconstrictor signaling in RGS2-deficient mice. *J. Clin. Invest.* **111**:445–452.
18. Zhang, W., et al. 2006. Selective loss of fine tuning of Gq/11 signaling by RGS2 protein exacerbates cardiomyocyte hypertrophy. *J. Biol. Chem.* **281**:5811–5820.
19. Tang, K.M., et al. 2003. Regulator of G-protein signaling-2 mediates vascular smooth muscle relaxation and blood pressure. *Nat. Med.* **9**:1506–1512.
20. Huang, J., Zhou, H., Mahavadi, S., Sriwai, W., and Murthy, K.S. 2007. Inhibition of Galphaq-dependent PLC-beta1 activity by PKG and PKA is mediated by phosphorylation of RGS4 and GRK2. *Am. J. Physiol. Cell Physiol.* **292**:C200–C208.
21. Takimoto, E., et al. 2005. Chronic inhibition of cyclic GMP phosphodiesterase 5A prevents and reverses cardiac hypertrophy. *Nat. Med.* **11**:214–222.
22. Zhang, R., et al. 2005. Calmodulin kinase II inhibition protects against structural heart disease. *Nat. Med.* **11**:409–417.
23. Fan, G., et al. 2005. A transgenic mouse model of heart failure using inducible Galpha q. *J. Biol. Chem.* **280**:40337–40346.
24. D'Angelo, D.D., et al. 1997. Transgenic Galphaq overexpression induces cardiac contractile failure in mice. *Proc. Natl. Acad. Sci. U. S. A.* **94**:8121–8126.
25. Hofmann, F., Feil, R., Kleppisch, T., and Schlossmann, J. 2006. Function of cGMP-dependent protein kinases as revealed by gene deletion. *Physiol. Rev.* **86**:1–23.
26. Taylor, M.S., et al. 2004. Inhibition of cGMP-dependent protein kinase by the cell-permeable peptide DT-2 reveals a novel mechanism of vasoregulation. *Mol. Pharmacol.* **65**:1111–1119.
27. Wilkins, B.J., et al. 2004. Calcineurin/NFAT coupling participates in pathological, but not physiological, cardiac hypertrophy. *Circ. Res.* **94**:110–118.
28. Zou, Y., et al. 2004. Mechanical stress activates angiotensin II type 1 receptor without the involvement of angiotensin II. *Nat. Cell Biol.* **6**:499–506.
29. Sadoshima, J., Xu, Y., Slayter, H.S., and Izumo, S. 1993. Autocrine release of angiotensin II mediates stretch-induced hypertrophy of cardiac myocytes in vitro. *Cell.* **75**:977–984.
30. Brancaccio, M., et al. 2003. Melusin, a muscle-specific integrin beta1-interacting protein, is required to prevent cardiac failure in response to chronic pressure overload. *Nat. Med.* **9**:68–75.
31. Hirota, H., et al. 1999. Loss of a gp130 cardiac muscle cell survival pathway is a critical event in the onset of heart failure during biomechanical stress. *Cell.* **97**:189–198.
32. Yamamoto, M., et al. 2003. Inhibition of endogenous thioredoxin in the heart increases oxidative stress and cardiac hypertrophy. *J. Clin. Invest.* **112**:1395–1406.
33. Hardt, S.E., and Sadoshima, J. 2004. Negative regulators of cardiac hypertrophy. *Cardiovasc. Res.* **63**:500–509.
34. Zhang, S., et al. 1998. RGS3 and RGS4 are GTPase activating proteins in the heart. *J. Mol. Cell. Cardiol.* **30**:269–276.
35. Owen, V.J., et al. 2001. Expression of RGS3, RGS4 and Gi alpha 2 in acutely failing donor hearts and end-stage heart failure. *Eur. Heart J.* **22**:1015–1020.
36. Jean-Baptiste, G., Yang, Z., and Greenwood, M.T. 2006. Regulatory mechanisms involved in modulating RGS function. *Cell. Mol. Life Sci.* **63**:1969–1985.
37. Abramow-Newerly, M., Roy, A.A., Nunn, C., and Chidiac, P. 2006. RGS proteins have a signalling complex: interactions between RGS proteins and GPCRs, effectors, and auxiliary proteins. *Cell Signal.* **18**:579–591.
38. Molkentin, J.D., et al. 1998. A calcineurin-dependent transcriptional pathway for cardiac hypertrophy. *Cell.* **93**:215–228.
39. Rahman, A., et al. 2002. Galpha (q) and Gbetagamma regulate PAR-1 signaling of thrombin-induced NF-kappaB activation and ICAM-1 transcription in endothelial cells. *Circ. Res.* **91**:398–405.
40. Abramow-Newerly, M., Roy, A.A., Nunn, C., and Chidiac, P. 2006. RGS proteins have a signalling complex: interactions between RGS proteins and GPCRs, effectors, and auxiliary proteins. *Cell Signal.* **18**:579–591.
41. Han, J., et al. 2006. RGS2 determines short-term synaptic plasticity in hippocampal neurons by regulating Gi/o-mediated inhibition of presynaptic Ca2+ channels. *Neuron.* **51**:575–586.

42. Anger, T., et al. 2007. RGS protein specificity towards Gq- and Gi/o-mediated ERK 1/2 and Akt activation, in vitro. *J. Biochem. Mol. Biol.* **40**:899–910.
43. Roy, A.A., et al. 2006. Up-regulation of endogenous RGS2 mediates cross-desensitization between Gs and Gq signaling in osteoblasts. *J. Biol. Chem.* **281**:32684–32693.
44. Zhang, M., et al. 2008. Expression, activity, and pro-hypertrophic effects of PDE5A in cardiac myocytes. *Cell Signal.* **20**:2231–2236.
45. Nagayama, T., et al. 2009. Sildenafil stops progressive chamber, cellular, and molecular remodeling and improves calcium handling and function in hearts with pre-existing advanced hypertrophy due to pressure overload. *J. Am. Coll. Cardiol.* **53**:207–215.
46. McKinsey, T.A., and Kass, D.A. 2007. Small-molecule therapies for cardiac hypertrophy: moving beneath the cell surface. *Nat. Rev. Drug Discov.* **6**:617–635.
47. Fiedler, B., et al. 2002. Inhibition of calcineurin-NFAT hypertrophy signaling by cGMP-dependent protein kinase type I in cardiac myocytes. *Proc. Natl. Acad. Sci. U. S. A.* **99**:11363–11368.
48. Gudi, T., et al. 2002. cGMP-dependent protein kinase inhibits serum-response element-dependent transcription by inhibiting rho activation and functions. *J. Biol. Chem.* **277**:37382–37393.
49. Li, P., et al. 2008. Atrial natriuretic peptide inhibits transforming growth factor beta-induced Smad signaling and myofibroblast transformation in mouse cardiac fibroblasts. *Circ. Res.* **102**:185–192.
50. Fiedler, B., et al. 2006. cGMP-dependent protein kinase type I inhibits TAB1-p38 mitogen-activated protein kinase apoptosis signaling in cardiac myocytes. *J. Biol. Chem.* **281**:32831–32840.
51. Osei-Owusu, P., et al. 2007. Regulation of RGS2 and second messenger signaling in vascular smooth muscle cells by cGMP-dependent protein kinase. *J. Biol. Chem.* **282**:31656–31665.
52. Gudi, T., Lohmann, S.M., and Pilz, R.B. 1997. Regulation of gene expression by cyclic GMP-dependent protein kinase requires nuclear translocation of the kinase: identification of a nuclear localization signal. *Mol. Cell. Biol.* **17**:5244–5254.
53. Gross, V., et al. 2005. Autonomic nervous system and blood pressure regulation in RGS2-deficient mice. *Am. J. Physiol. Regul. Integr. Comp. Physiol.* **288**:R1134–R1142.
54. Oliveira-dos-Santos, A.J., et al. 2000. Regulation of T cell activation, anxiety, and male aggression by RGS2. *Proc. Natl. Acad. Sci. U. S. A.* **97**:12272–12277.
55. DeBosch, B., et al. 2006. Akt1 is required for physiological cardiac growth. *Circulation.* **113**:2097–2104.
56. De Windt, L.J., Lim, H.W., Haq, S., Force, T., and Molkentin, J.D. 2000. Calcineurin promotes protein kinase C and c-Jun NH2-terminal kinase activation in the heart. Cross-talk between cardiac hypertrophic signaling pathways. *J. Biol. Chem.* **275**:13571–13579.
57. Takimoto, E., et al. 2005. cGMP catabolism by phosphodiesterase 5A regulates cardiac adrenergic stimulation by NOS3-dependent mechanism. *Circ. Res.* **96**:100–109.